

## **Time-Varying Manual Control Identification in a Stall Recovery Task under Different Simulator Motion Conditions**

Alexandru Popovici, San Jose State University; Peter M. T. Zaal, San Jose State University; Marc A. Pieters, San Jose State University

This paper adds data to help develop simulator motion guidelines for stall recovery training by identifying time-varying manual control behavior in a stall recovery task under different simulator motion conditions. A study was conducted in the NASA Ames Vertical Motion Simulator, where seventeen general aviation pilots performed a stall recovery task. Pilots had to follow a flight director through four stages of the stall recovery task. A time-varying identification method was used to quantify how pilots weigh position and velocity information throughout different stages of the task, in both roll and pitch. Four motion configurations were used: no motion, generic hexapod motion, enhanced hexapod motion and full motion. Pilot performance was highest for the enhanced hexapod and full motion conditions in both roll and pitch, and the lowest for the condition with no motion. The time-varying identification method revealed that, in the roll axis, pilot position gain did not significantly change between time segments, but was the lowest for the condition with no motion. The pilot velocity gain was significantly different between motion conditions, the largest difference being found at the beginning of the stall. The enhanced hexapod motion condition had the highest pilot velocity gain. In the pitch axis, the pilot position gain was significantly different between time segments but not between motion conditions. The pitch pilot velocity gain was highest for the full motion condition and increased at the beginning of the stall, but did not change significantly for the other motion conditions. Overall, pilot control behavior under enhanced hexapod motion was more similar to that under full aircraft motion compared to standard hexapod motion. This indicates that motion cueing on hexapod simulators might be improved for stall recovery training by using the enhanced hexapod motion developed in previous experiments.

# TIME-VARYING MANUAL CONTROL IDENTIFICATION IN A STALL RECOVERY TASK UNDER DIFFERENT SIMULATOR MOTION CONDITIONS

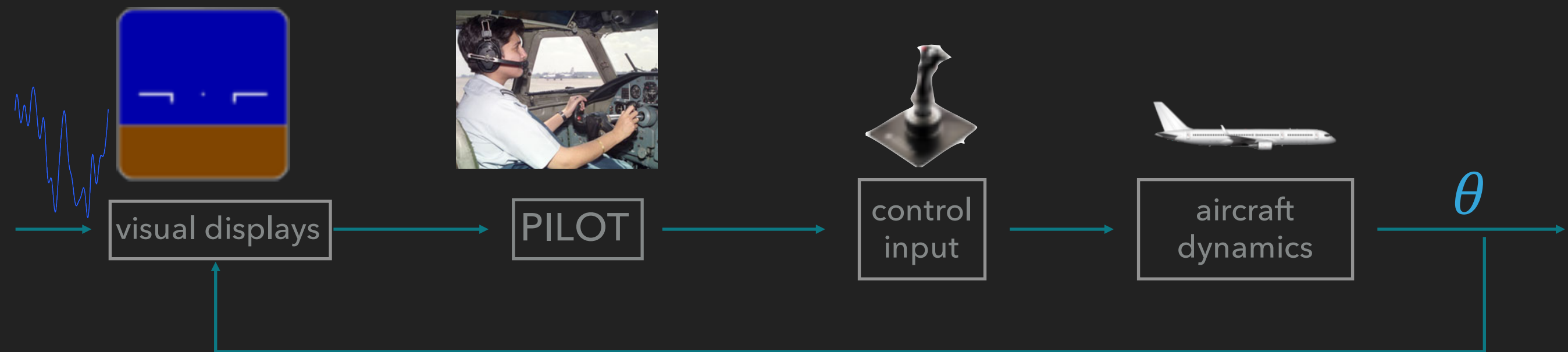
*AIAA-2018-2936*

A. POPOVICI, P. ZAAL, M. PIETERS

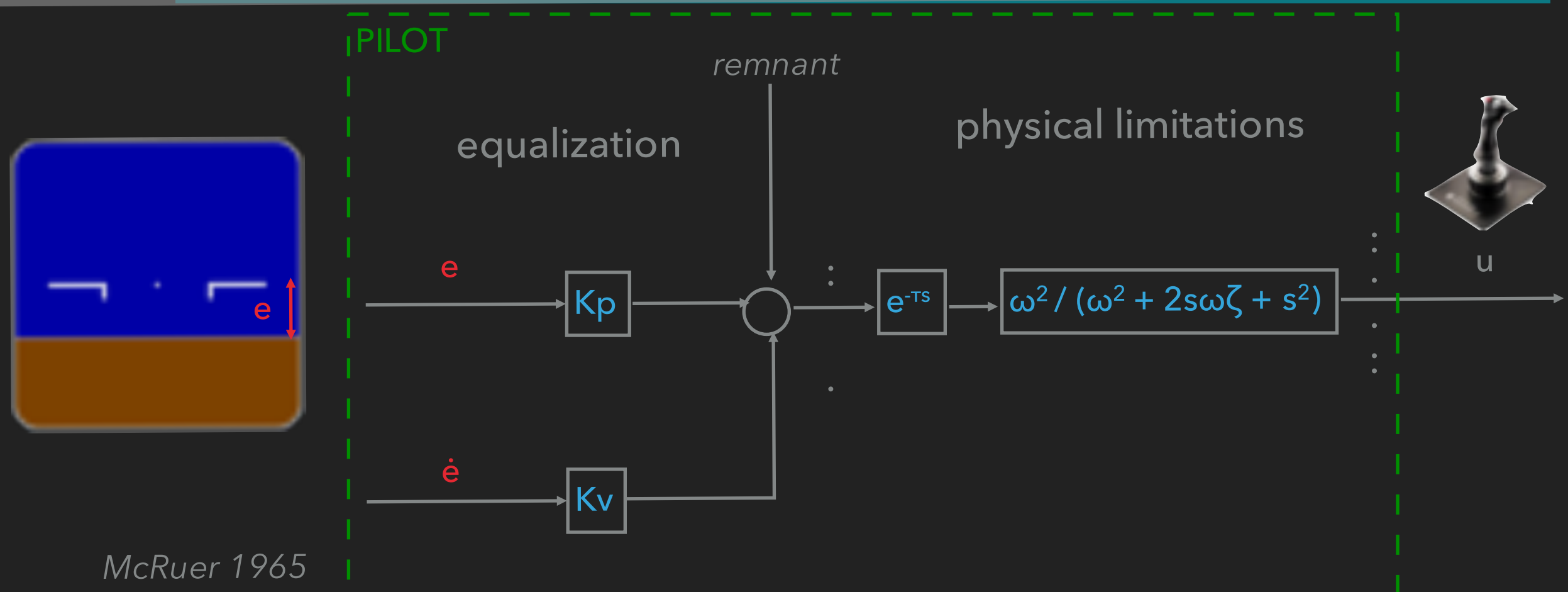
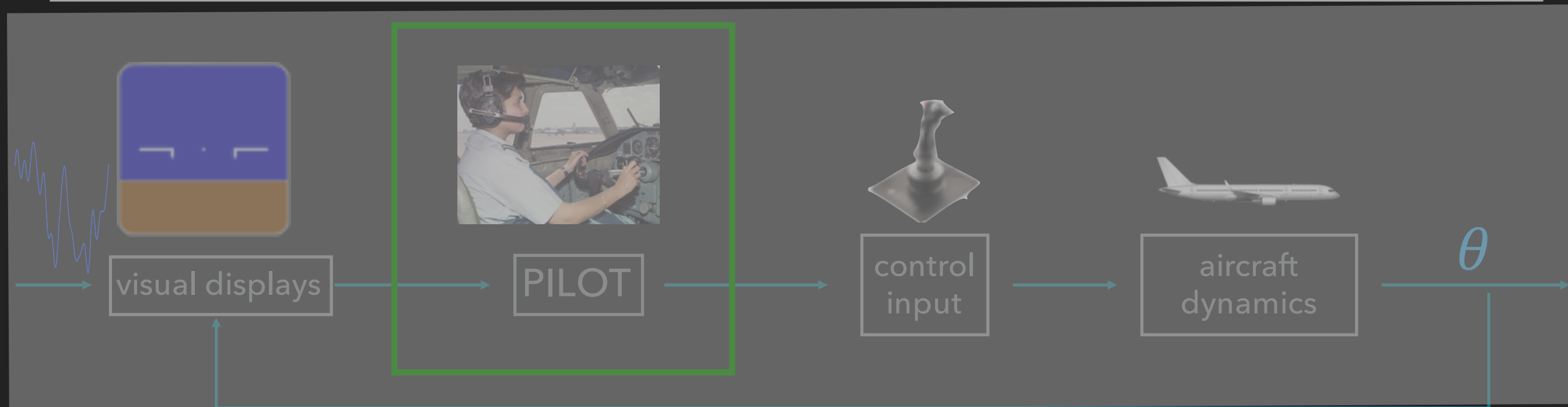


SAN JOSÉ STATE  
UNIVERSITY

# BACKGROUND (1) – CYBERNETICS



# BACKGROUND (1) - CYBERNETICS



McRuer 1965

## BACKGROUND (2) – MOTION CUEING FOR STALL RECOVERY



### single-axis, time-invariant tasks

Effects of False Tilt Cues on the  
Training of Manual Roll Control Skills  
AIAA - 2015 - 0655

Effects of Heave Motion Components  
on Pitch Control Behavior  
AIAA - 2016 - 3371

Effects of Motion Cues on the  
Training of Multi-Axis Manual Control  
Skills  
AIAA - 2017 - 3473

⋮

Time-Varying Manual Control  
Identification in a Stall Recovery Task  
Under Different Simulator Motion  
Conditions  
AIAA - 2018 - 2936

*Time-Varying Pilot Control Behavior  
Identification using MLE  
AIAA - 2012 - 4793*

*Multi-Axis Tracking Tasks with Time-  
Varying Motion  
AIAA - 2014 - 0810*

*Time-Varying Pilot Control  
Identification using Kalman Filtering  
AIAA - 2017 - 3666*

### multi-axis, time-varying tasks



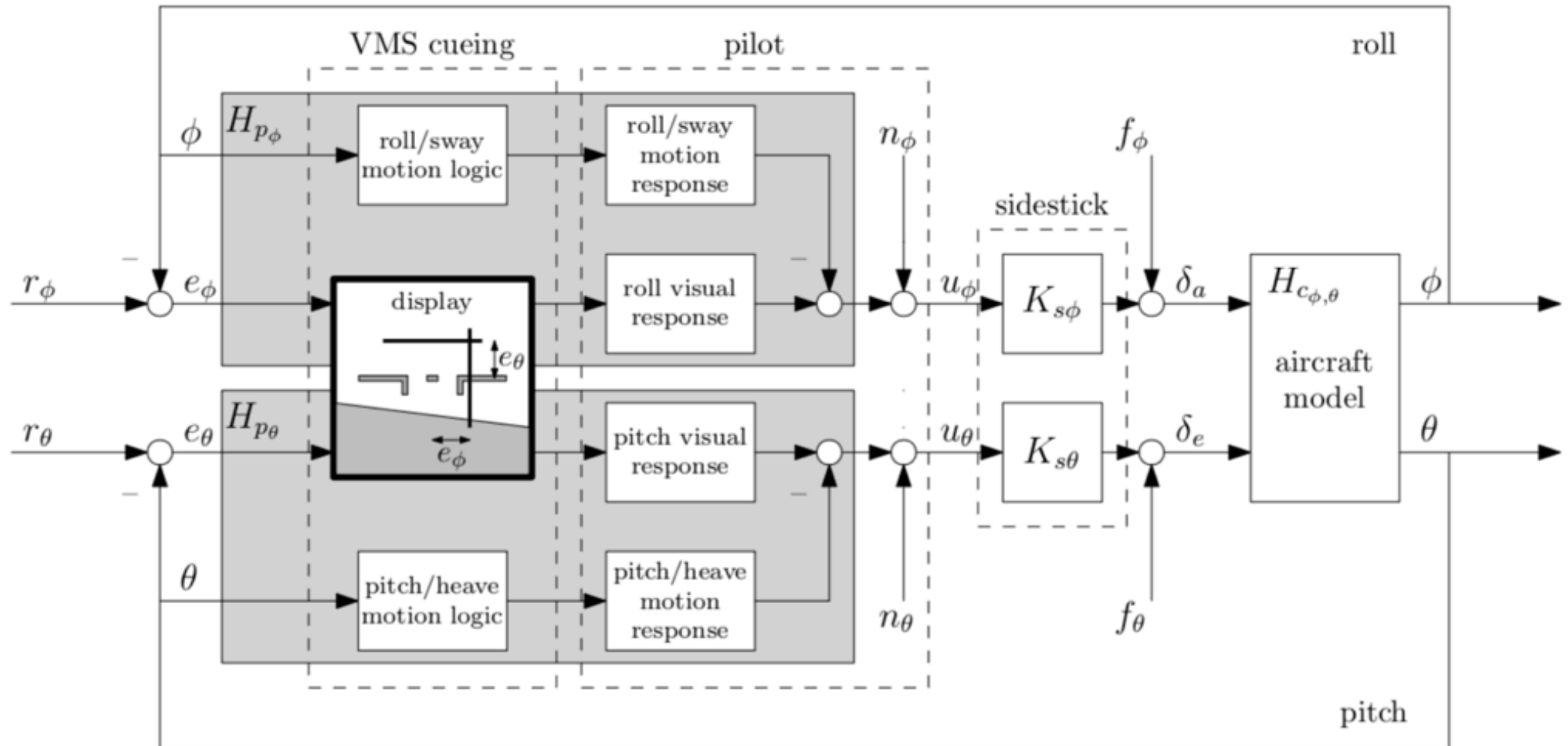
## RESEARCH QUESTIONS – STALL RECOVERY TASK

---

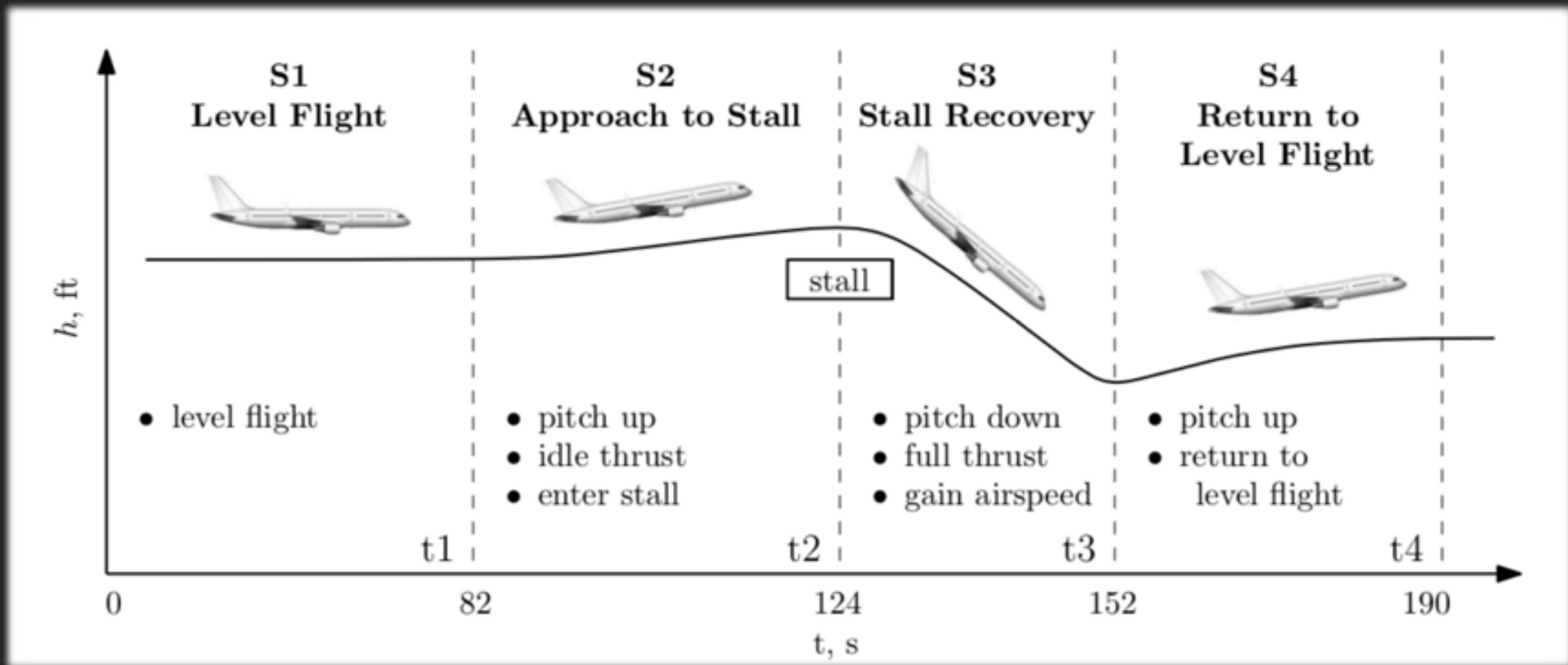
1. What are the effects of different simulator motion settings on human manual control?
2. How do pilots adapt their control strategies through different stages of stall recovery?
3. Are differences in motion the same during different stages of stall recovery?



# DOUBLE-AXIS COMPENSATORY TASK









No Motion(NM)

*no motion cues*

Generic Hexapod (GH)

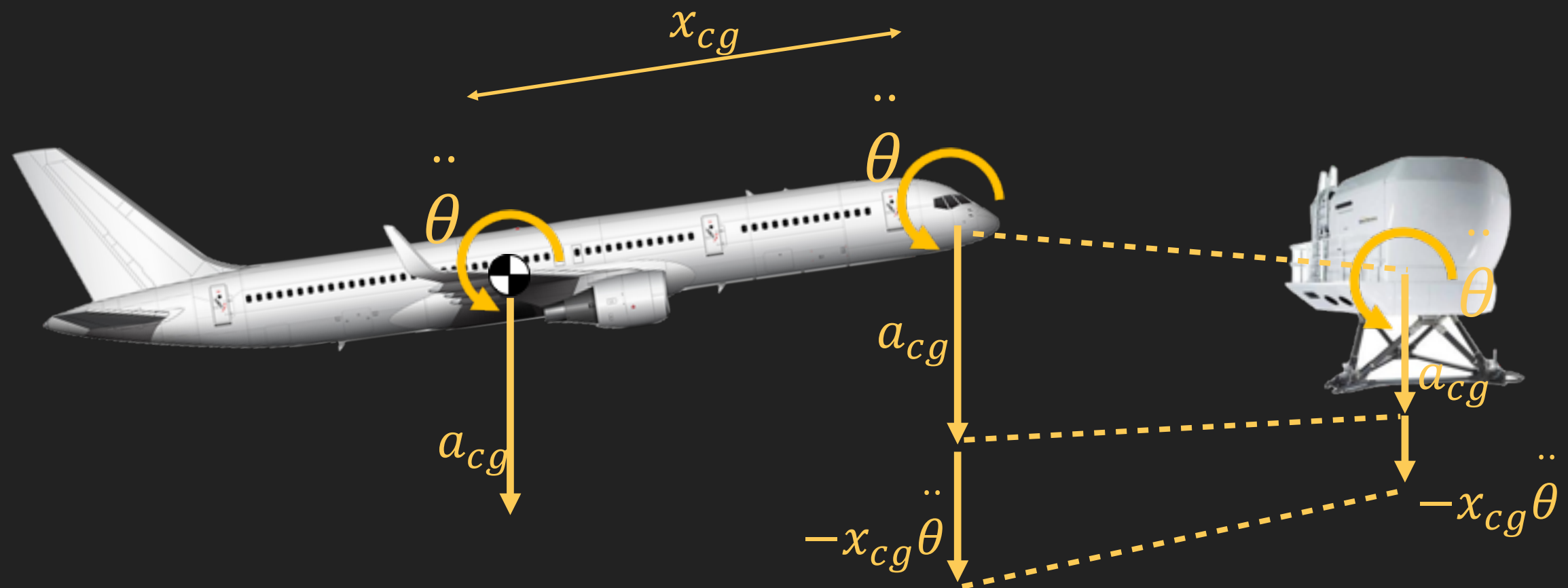
*typical motion by training  
hexapod simulators*

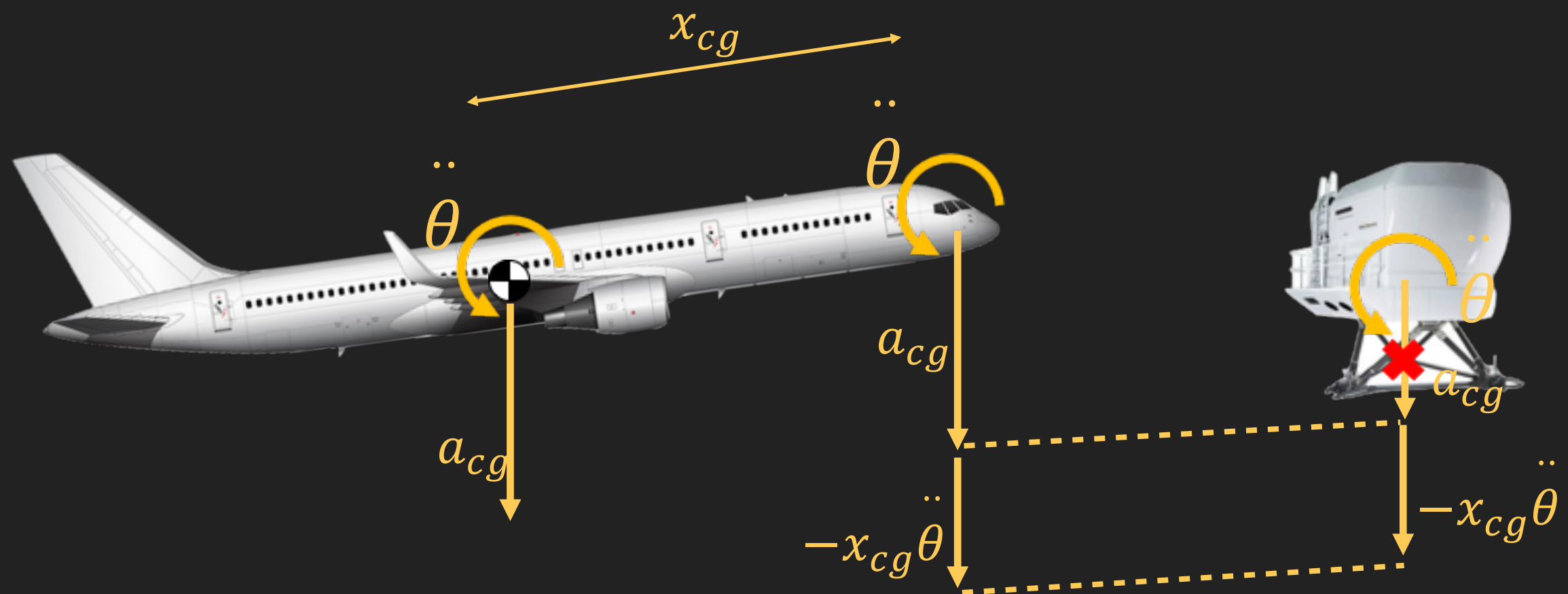
Enhanced Hexapod (EH)

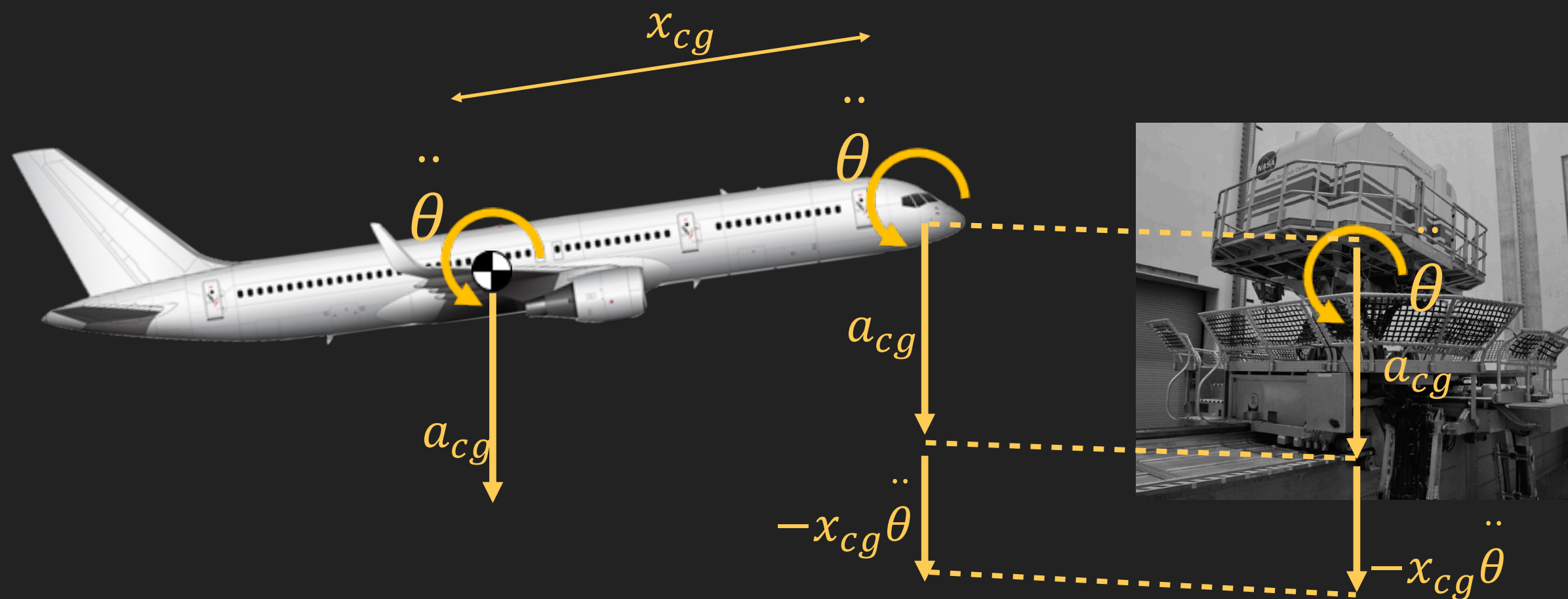
*eliminate translational  
acceleration of c.g.*

Full Motion (FM)

*full aircraft motion*

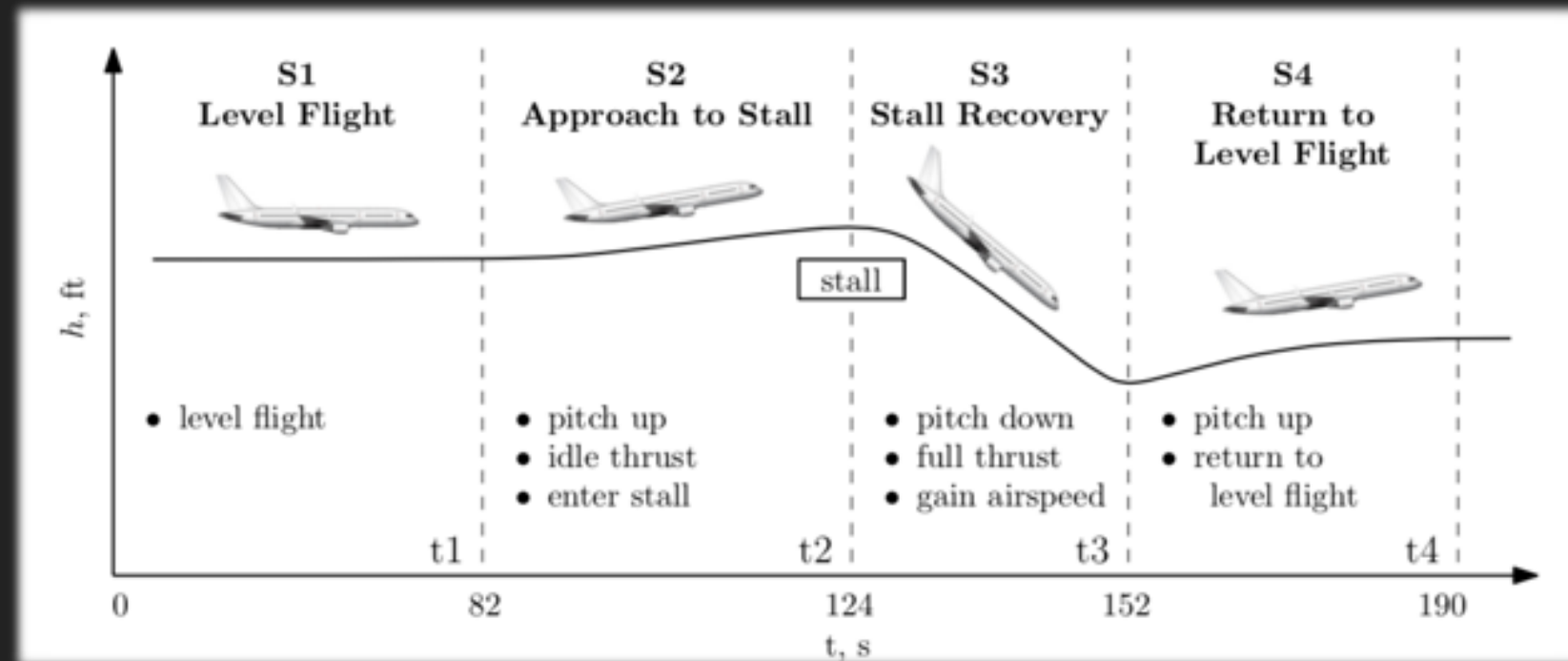


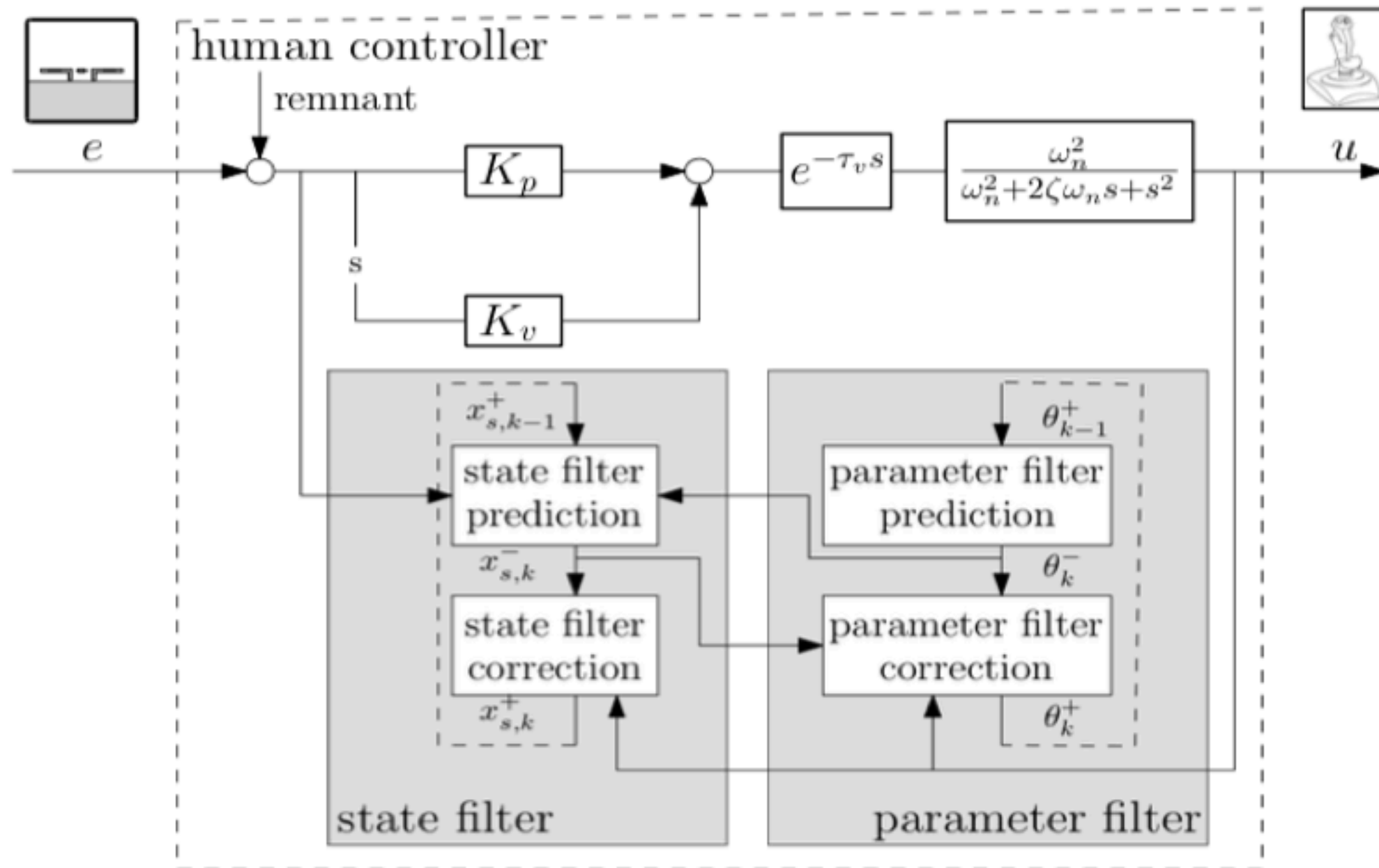




# EXPERIMENT DESIGN

- ▶ 17 general aviation pilots
- ▶ 32 (8x4 runs)
- ▶ Vertical Motion Simulator
- ▶ GTM model
- ▶ dependent measures
  - ▶ human manual control parameters
  - ▶ open-loop stability and phase margin
  - ▶ RMS error and control activity

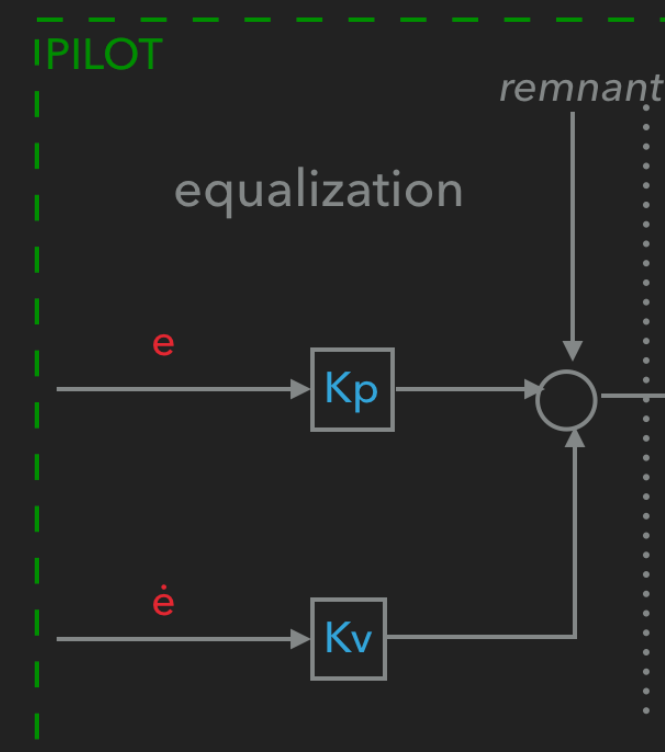
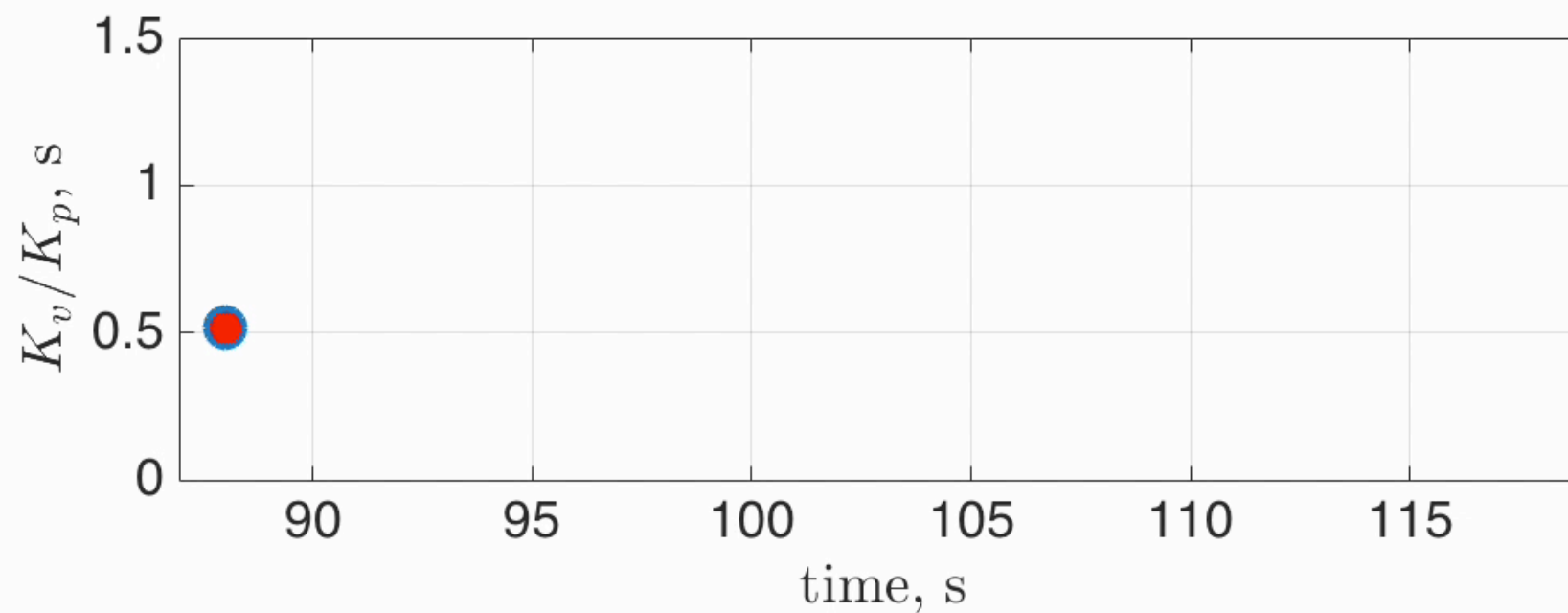
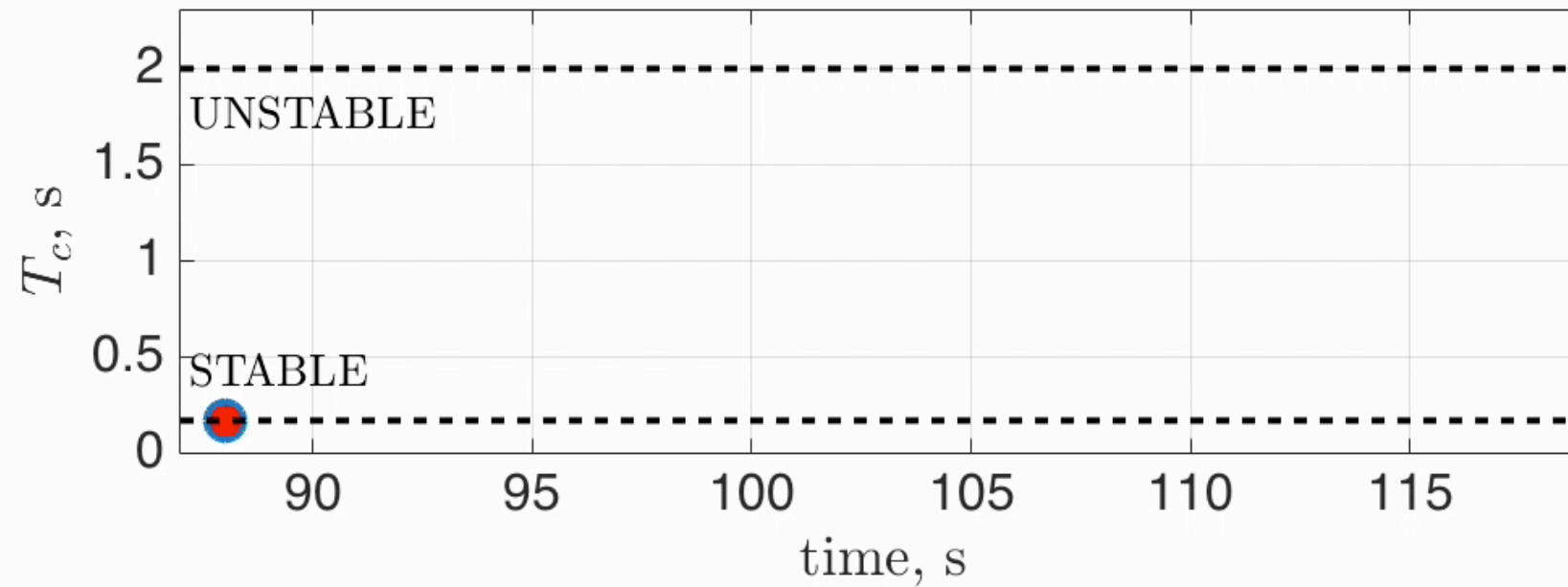




- two extended Kalman filters running in parallel
- **state filter**: estimates equalization parameters
- **parameter filter**: estimates neuromuscular parameters
- constant time delay

# DUAL EXTENDED KALMAN FILTER – EXAMPLE

$$H_c(s, t) = \frac{K_c}{s(T_c(t)s + 1)}$$

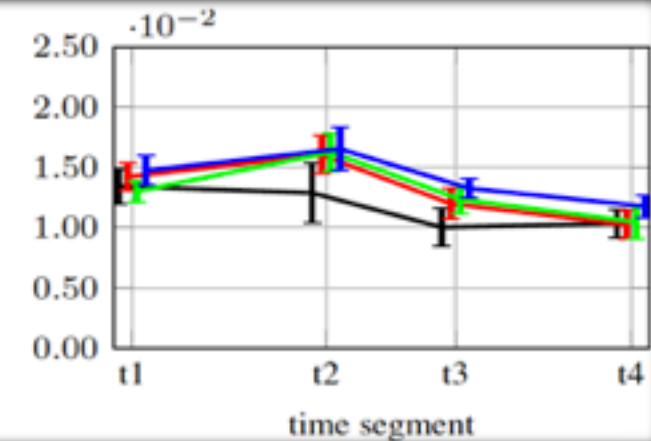
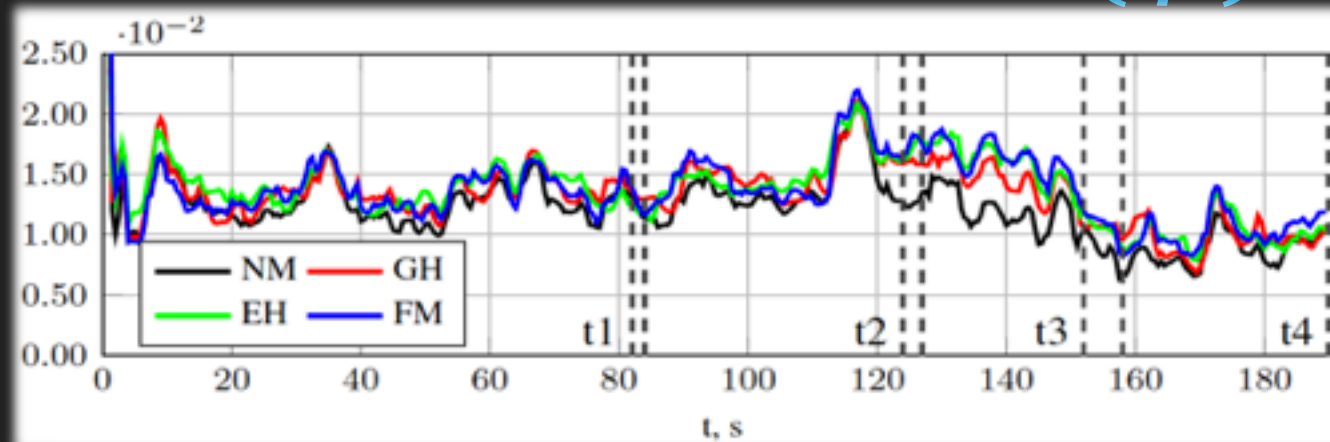




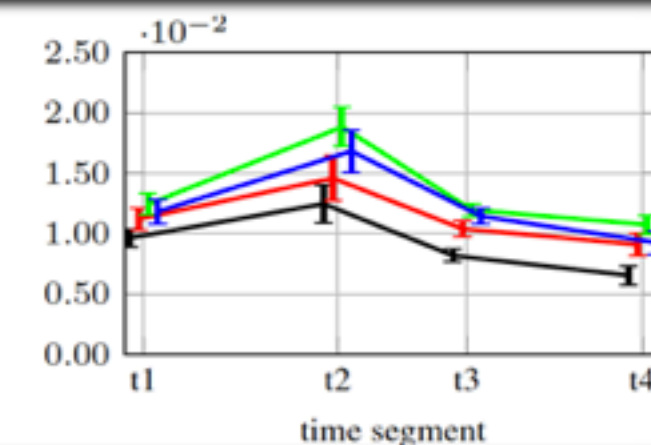
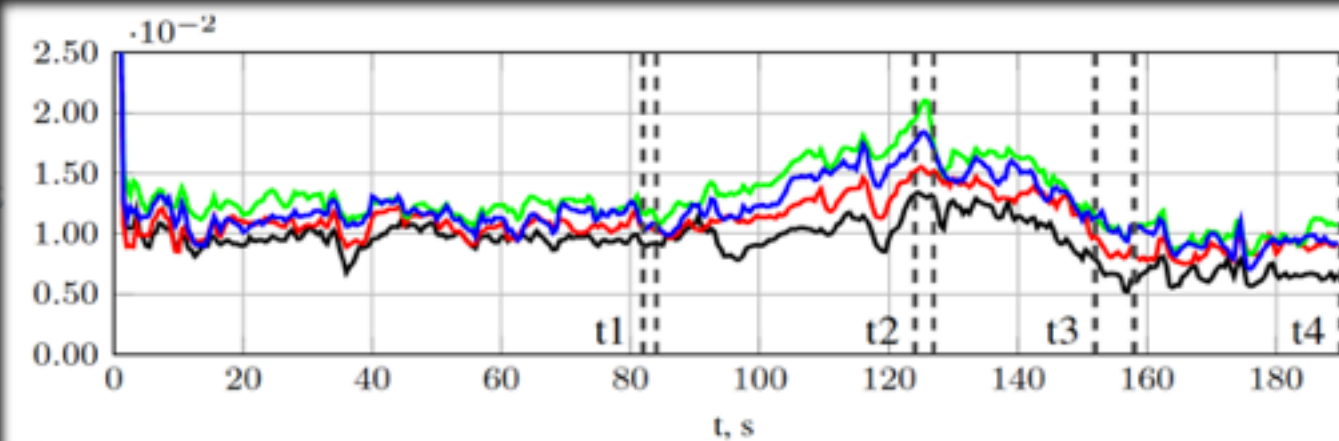
# RESULTS – POSITION AND VELOCITY GAINS

## Roll( $\phi$ )

### $K_p$



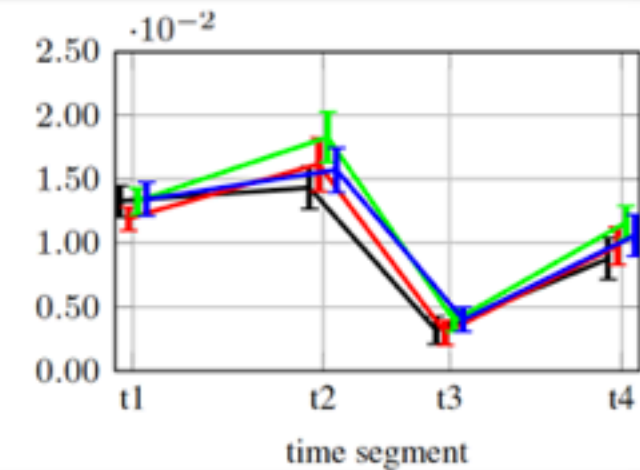
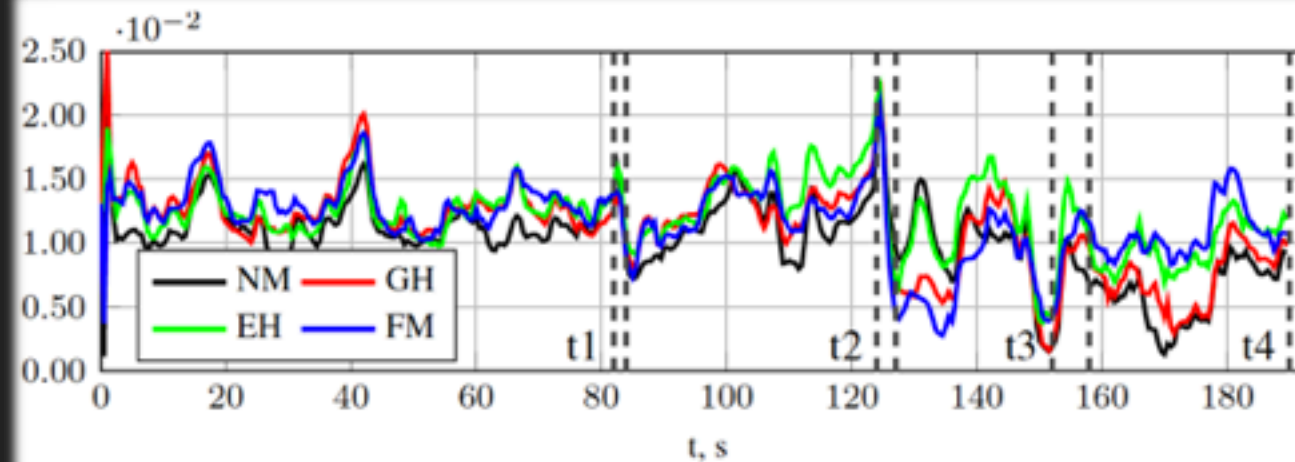
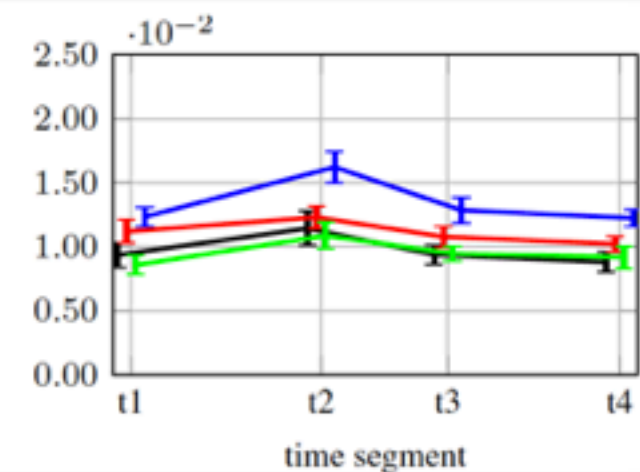
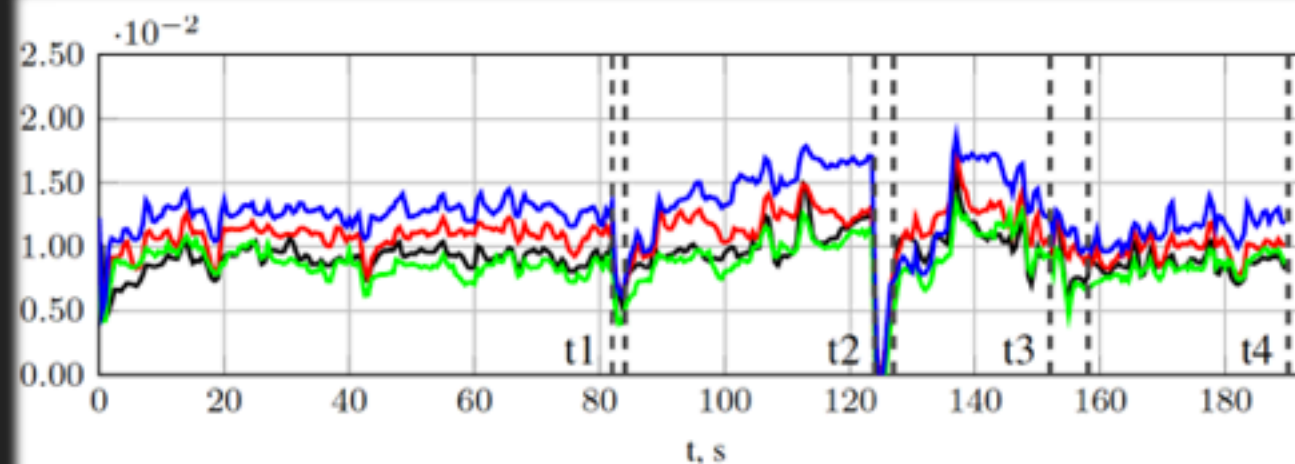
### $K_v$



- position gain:
  - lower for NM in t2(stall) and t3(dive)
  - no differences between time segments
- velocity gain:
  - highest for EH
  - increases towards stall (t2); lower after recovery (t4)
  - highest difference at stall (t2)



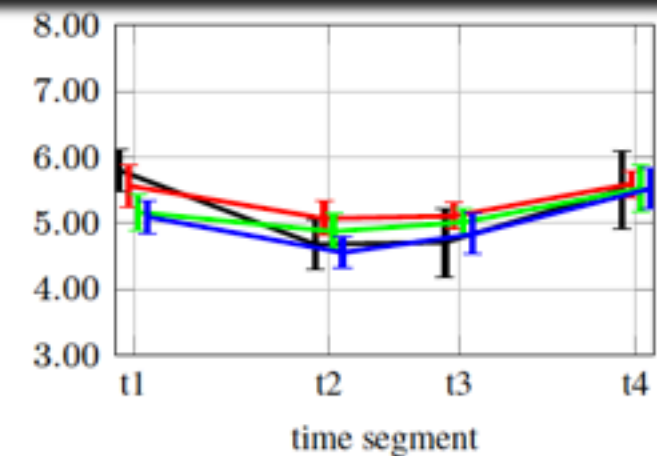
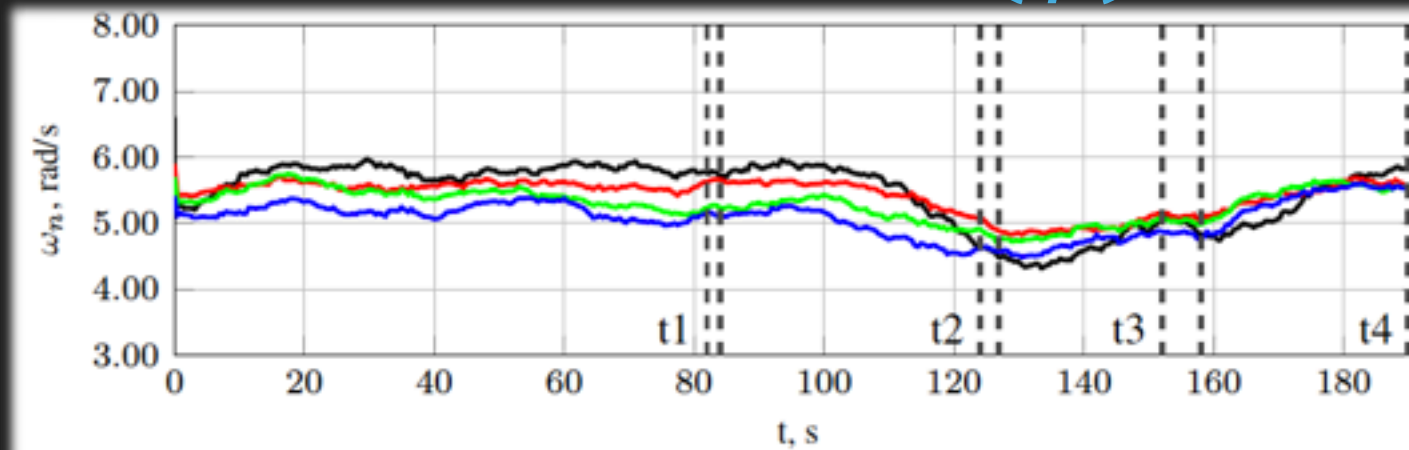
## RESULTS – POSITION AND VELOCITY GAINS

 $Pitch(\theta)$  $K_p$  $K_v$ 

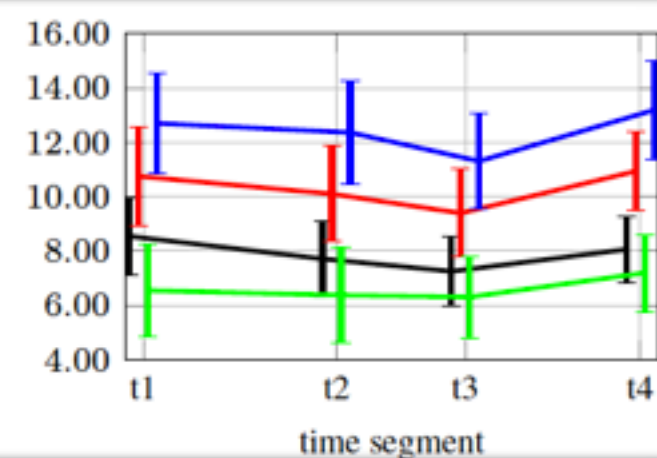
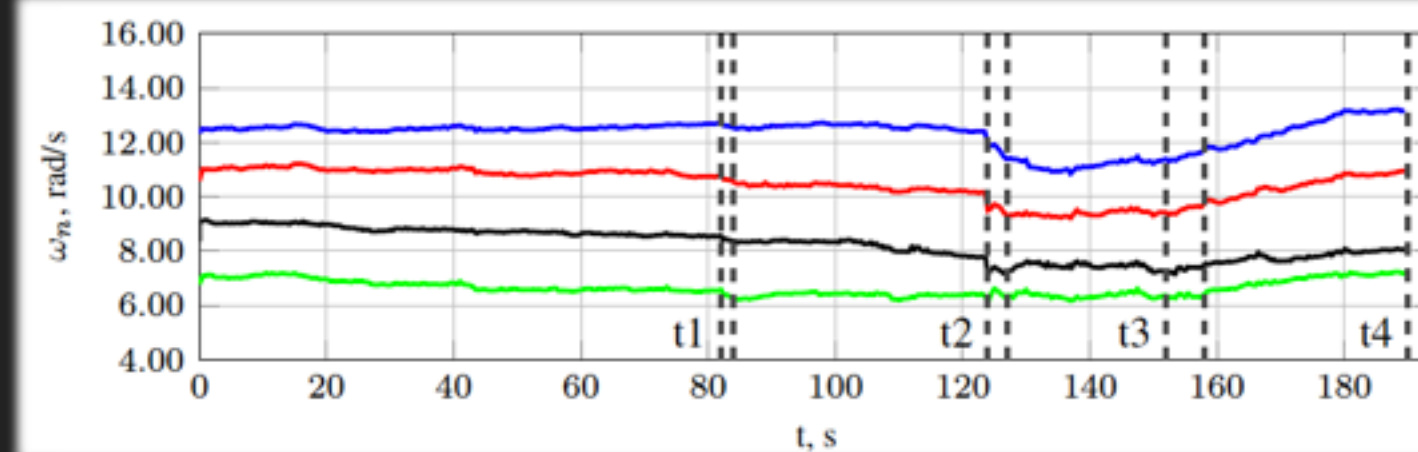
- position gain:
  - no difference between motion conditions
  - decreased at (t3)
- velocity gain:
  - highest for FM
  - higher at the beginning of stall for FM

# RESULTS – NEUROMUSCULAR FREQUENCY

## Roll( $\phi$ )

 $\omega_n$ 


## Pitch( $\theta$ )

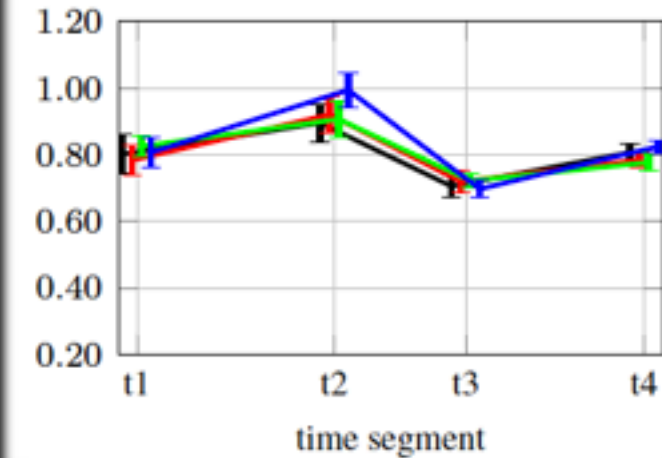
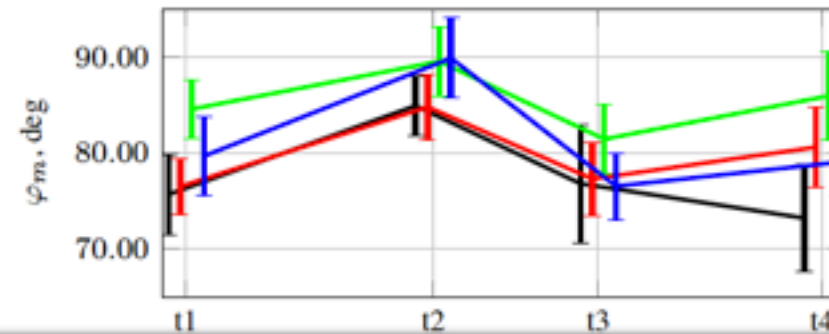
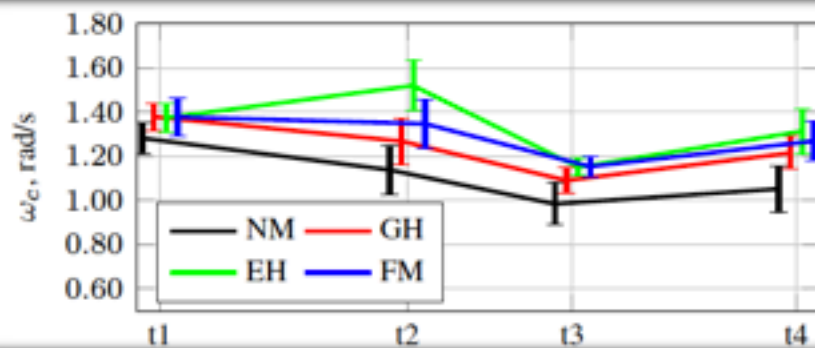
 $\omega_n$ 


- roll:
  - no difference between motion conditions
  - decreases in stall and dive
- pitch:
  - highest for FM, lowest for NM
  - decreases in stall and dive

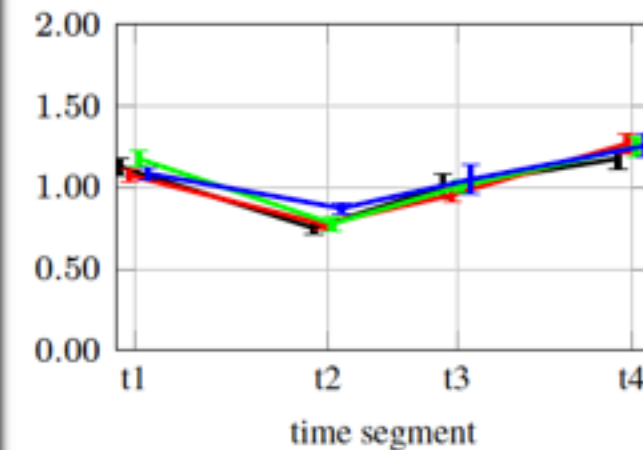
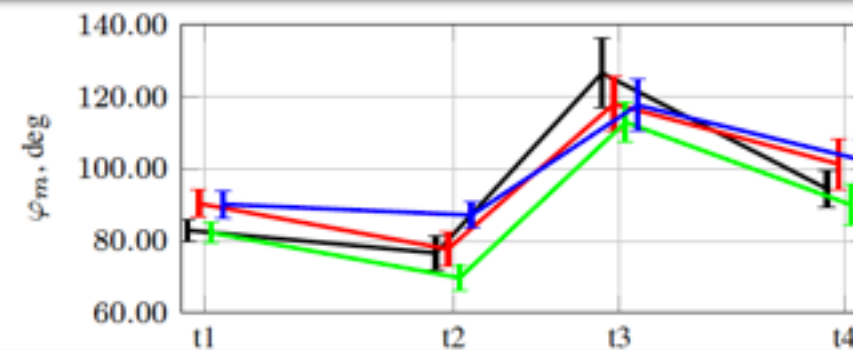
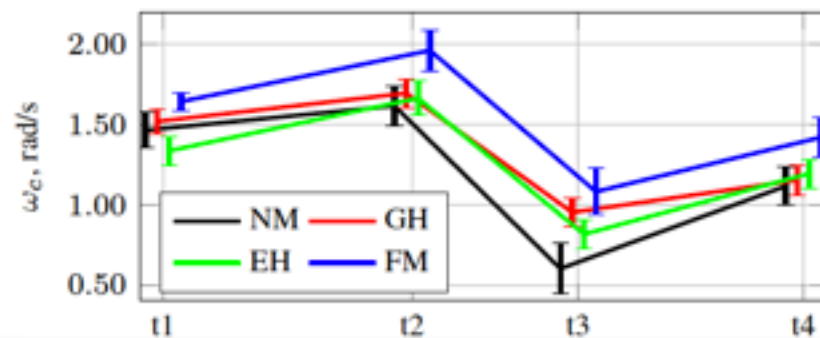
# RESULTS – OPEN-LOOP CHARACTERISTICS

 $\phi$ 
 $\omega_c$ 
 $\varphi_m$ 

dynamics crossover frequency


 $\theta$ 
 $\omega_c$ 
 $\varphi_m$ 

dynamics crossover frequency



- roll:
  - crossover frequency higher with motion
  - crossover frequency lowest in the dive(t3)
  - phase margin highest for EH
  - phase margin highest at stall (t2)

- pitch:
  - crossover frequency highest for FM
  - crossover frequency lowest at the end of the dive(t3)
  - phase margin lowest for EH
  - highest at the end of dive(t3)

- ▶ multi-axis time-varying pilot identification in a stall recovery task
- ▶ the enhanced hexapod condition was the closest to the full motion condition
- ▶ pilot manual control behavior was different in roll and pitch axes
- ▶ differences in motion larger closer to stall point
- ▶ adaptive motion cueing





# TIME-VARYING MANUAL CONTROL IDENTIFICATION IN A STALL RECOVERY TASK UNDER DIFFERENT SIMULATOR MOTION CONDITIONS



A. POPOVICI, P. ZAAL, M. PIETERS



SAN JOSÉ STATE  
UNIVERSITY

**EXTRA SLIDES**



## STATE SPACE REPRESENTATION (1)

$$(K_p(t) + K_v(t)s)e^{-\tau_v s} \frac{\omega_n^2(t)}{s^2 + 2\zeta_n(t)\omega_n(t)s + \omega_n^2(t)}$$

$$\begin{aligned}\dot{\mathbf{x}}_s(t) &= \mathbf{f}(\mathbf{x}_s(t), e(t), \boldsymbol{\theta}(t)) + \mathbf{w}_s(t) \\ u(t) &= g(\mathbf{x}_s(t), \boldsymbol{\theta}(t)) + v(t)\end{aligned}$$

$$\begin{aligned}\dot{\boldsymbol{\theta}}(t) &= \mathbf{w}_p(t) \\ u(t) &= g(\mathbf{x}_s(t), \boldsymbol{\theta}(t)) + v(t)\end{aligned}$$

$$\begin{aligned}\mathbf{x}_s &= \begin{bmatrix} x_{s,1} & x_{s,2} & x_{s,3} & x_{s,4} & x_{s,5} & K_p & K_v \end{bmatrix}^T \\ \boldsymbol{\theta} &= \begin{bmatrix} \omega_n & \zeta_n & \tau_v \end{bmatrix}^T\end{aligned}$$

## STATE SPACE REPRESENTATION (2)

$$Q_p = \text{diag}([0.1\omega_{n,0} \ 0.1\zeta_{n,0} \ 0.1\tau_{v,0}])$$

$$Q_s(k) = \text{diag} \left( \begin{bmatrix} 0 & 0 & 0 & 0 & q^2\sigma_{e(k-5/\Delta t:k)}^2 & K_{p,0} & K_{v,0} \end{bmatrix} \right)$$

$$f(\mathbf{x}_s, e, \boldsymbol{\theta}) = \begin{bmatrix} x_{s,2} \\ x_{s,3} \\ x_{s,4} \\ x_{s,5} \\ e - x_{s,3}(12\omega_n^2\tau_v^2 + 120\zeta_n\omega_n\tau_v + 120)/\tau_v^3 - x_{s,2}(60\tau_v\omega_n^2 + 240\zeta_n\omega_n)/\tau_v^3 - \\ \dots - x_{s,4}(\omega_n^2\tau_v^3 + 24\zeta_n\omega_n\tau_v^2 + 60\tau_v)/\tau_v^3 - x_{s,5}(2\zeta_n\omega_n\tau_v^3 + 12\tau_v^2)/\tau_v^3 - 120x_{s,1}\omega_n^2/\tau_v^3 \\ 0 \\ 0 \end{bmatrix}$$

$$g(\mathbf{x}_s, \boldsymbol{\theta}) = \begin{bmatrix} x_{s,3}(12K_p\omega_n^2\tau_v^2 - 60K_v\omega_n^2\tau_v)/\tau_v^3 - K_v\omega_n^2x_{s,5} + x_{s,2}(120K_v\omega_n^2 - 60K_p\omega_n^2\tau_v)/\tau_v^3 - \\ \dots - x_{s,4}(K_p\omega_n^2\tau_v^3 - 12K_v\omega_n^2\tau_v^2)/\tau_v^3 + 120K_p\omega_n^2x_{s,1}/\tau_v^3 \end{bmatrix}$$

Parameter filter prediction:

$$\theta_k^- = \theta_{k-1}^+$$

$$P_{p,k}^- = \Phi_{p,k-1} P_{p,k-1}^+ \Phi_{p,k-1}^T + \Gamma_{p,k-1} Q_p \Gamma_{p,k-1}^T$$

State filter prediction:

$$\mathbf{x}_{s,k}^- = \mathbf{x}_{s,k-1}^+ + f(\mathbf{x}_{s,k-1}^+, e_{k-1}, \theta_k^-) \Delta t$$

$$P_{s,k}^- = \Phi_{s,k-1} P_{s,k-1}^+ \Phi_{s,k-1}^T + \Gamma_{s,k-1} Q_s \Gamma_{s,k-1}^T$$

State filter (partial) correction:

$$K_{s,k} = P_{s,k}^- G_{s,k}^T [G_{s,k} P_{s,k}^- G_{s,k}^T + R]^{-1}$$

$$P_{s,k}^+ = (I - K_{s,k} G_{s,k}) P_{s,k}^- (I - K_{s,k} G_{s,k})^T + K_{s,k} R K_{s,k}^T$$

Parameter filter correction:

$$K_{p,k} = P_{p,k}^- (G_{p,k}^{tot})^T [G_{p,k}^{tot} P_{p,k}^- (G_{p,k}^{tot})^T + R]^{-1}$$

$$\theta_k^+ = \theta_k^- + K_{p,k} [u_k - g(\mathbf{x}_{s,k}^-, e_k, \theta_k^-)]$$

$$P_{p,k}^+ = (I - K_{p,k} G_{p,k}^{tot}) P_{p,k}^- (I - K_{p,k} G_{p,k}^{tot})^T + K_{p,k} R K_{p,k}^T$$

